Proceedings of the Institute of Acoustics

PRELIMINARY RESULTS FROM TECHNIQUES TO DETERMINE IN SITU MEDIUM SPEED OF SOUND USING A SYNTHETIC APERTURE SONAR

JL Prater Naval Surface Warfare Center Panama City Division, Panama City, Florida, USA
TM Marston Applied Physics Laboratory, University of Washington, Seattle, Washington, USA

1 INTRODUCTION

Synthetic Aperture Sonar (SAS) systems require accurate speed of sound (c) measurements to produce focused imagery. Now that systems are being developed to operate at long ranges and in more complex environments, tools are needed to determine or verify the *in situ* medium c value at ranges matching that of the system. It has previously been noted that the range-variance of quadratic defocusing induced by sound-speed error (*e.g.* linear in range) is the same as that induced by forward velocity offsets[1]. *In-situ* estimations of *c* that rely on focus maximization[2] are subject to this ambiguity unless it is known *a-priori* that along-track displacement error is negligible. To resolve this ambiguity the authors propose a technique for RPC-based forward velocity estimation that is insensitive to erroneous values of *c*, potentially increasing the accuracy of *in-situ* *c* estimates found by observation of range-variant quadratic defocusing.

Linearly range-variant quadratic focusing errors were observed in SAS imagery spanning a variety of environmental conditions. An autofocus algorithm was developed for estimation of the linearly range variant quadratic phase error, and this algorithm adequately resolved the focusing aberrations. As stated previously however, this method cannot be used to differentiate between errors in along-track displacement and speed of sound. As an alternative to the autofocusing algorithm an independent method was developed that uses redundant phase center (RPC) data to determine small displacement errors in the along-track direction. Though largely insensitive to *c* this method was still observed to significantly enhance the focus of a large number of the scenes containing focusing aberrations. This led to the conclusion that velocity offsets were responsible for image defects in some of the cases, while sound-speed errors were responsible in others. Furthermore, when the two methods are used in combination the ambiguity between along-track error and sound-speed error can be resolved and a more accurate *in-situ* estimation of c made. A brief overview of the RPC based along-track displacement measurement method and the autofocus algorithms are discussed, and the technique for combining the approaches to estimate c is presented. The hypothesis that speed of sound can be measured with the aforementioned techniques is evaluated with data samples from environments with differing c estimates (c ranging from ~1450-1530m/s). The results as well as future efforts to calibrate the method or otherwise determine the accuracy of the measurements are discussed.

2 SONAR-BASED ESTIMATION OF C

2.1 Along-track motion estimation

SAS image formation requires precise localization of receive array elements to maintain coherence across the aperture. Range axis and vertical sonar array displacement are routinely measured with RPC data[1,3,4]. In this technique, data collected from sonar element positions that overlap in space but across consecutive pings is compared. The relative delay observed between the consecutive pings is used to determine range-axis and vertical array displacement. Previous attempts to determine forward velocity from RPC analysis often relied on comparing relative measures of correlation between adjacent RPC pairs[1] (*i.e.* correlate the correctly matched pair with adjacent elements that do not overlap in space precisely similar to A_n of Ping n+1 with A_1 of Ping n in Figure 1). This technique is considerably less precise compared with range axis correlation measurements due to the relatively low correlation between adjacent channels and lacks the precision necessary for along-track motion compensation.

Figure 1: An example of array element positions for two consecutive pings as used for RPC analysis and an example of the squinted beams used in the proposed along-track RPC approach where two adjacent RPC channels are summed to provide squinted RPC beams at equivalent angles both forward and aft of broadside (A) and A geometric representation of the along-track RPC technique (B).. The RPC phase center for the initial ping is located at (0,0) and the center for the following ping is at (Δx,Δy). The fore and aft squinted beams are shown with distances to point targets at (x,y) and (-x,y) are indicated.

An analysis technique is possible to determine along-track position with precision similar to that of the range-axis measurements by forming new RPC beam pairs at off-broadside angles (Figure 1A). In this technique, adjacent elements are summed and squinted fore and aft of broadside. The data from the squinted pairs is compared over consecutive pings to determine displacement similar to that for broadside range-axis analysis. The deviation in path lengths to some point target at (x,y) for the forward case or (-x,y) in the aft case are determined through correlation analysis: ΔR_a for the aft displacement, and ΔR_f for the forward beam displacement (Figure 1B). From the geometry illustrated in Figure 1B, we can see that the path length between the Ping n+1 array elements and the point targets can be expressed by (1) for the forward case and (2) for the aft case.

(1)
(2)

The difference of (1) and (2) can be simplified to solve for Δx, and $R\sin(\Theta)$ can be substituted for x to yield (3) which expresses the deviation in along-track position from ideal in terms of the RPC displacements, the slant range used for correlation analysis, and the squint angle.

(3)

2.2 Sensitivity of along-track position measurement to error in c

Equation (3) is not independent of c because, as with most sonar-based displacement measurements, conversion of the time-domain data to distance requires knowledge of the speed of sound. However, an analysis of the error associated with uncertainty in c can demonstrate that the Δx measurement in (3) is not sensitive to error in c. Consider that measurement of R is determined by the time-of-flight to the point object (t) and displacements ΔR_a and ΔR_f are determined by observed time delays in the correlation analysis (τ_a τ_f). Each time measurement is converted to distance by multiplying by c/2 (to adjust for 2-way path length). These relationships can be substituted into equation 3 to yield an estimate of Δx that is based on the time-scaled parameters (4).

(4)

The term Θ is replaced with Θ_a to indicate that the correlation results are dependent on the realized squint angle rather than the intended angle.

The true c value is unknown, but the approximate value (c_i) deviates from the true value by some ratio ε (5).

(5)

This relationship between Θ and Θ_a can be determined from an evaluation of the process used to squint the RPC pair. To squint the RPC channels, they are summed with a phase shift applied to ensure that incoming waves from the desired angle are coherent under a plane-wave assumption.

The applied phase shift Φ (6) is dependent on both the desired angle (Θ), the physical separation between the receive elements (du), and the frequency (f_0).

(6)

Considering that c_i is used at the time of calculation (*i.e.* Φ contains error associated with the use of c_i), the actual angle (Θ_a) will deviate from the desired angle by the ratio expressed in (7).

(7)

Substituting this result in (4) yields an expression independent on the actual c value but dependent on c_i and Θ rather than Θ_a. Therefore, it can be demonstrated that Δx estimates are independent of c as long as the estimate of c is valid. (*i.e.* c_i must be close enough to ensure that the squint angle is not steep enough to allow main-lobe aliasing).

(8)

The relationship between Δx and c is illustrated in Figure 2 which shows the observed error in along-track displacement determined via the RPC analysis approach described above for $c_i = c_s \pm 60$ m/s at 20 m/s intervals. The error ratio shown is the ratio of measured ping-to-ping displacement compared with ideal displacement (). This ratio is analogous to ε except that it describes the error associated with array spacing that contributes to quadratic phase error. The figure illustrates the point that the RPC-based results are independent of c_i because the measured along-track error is near constant (0.9813 ± 0.0001) while ε is allowed to vary from ~0.96 to ~1.04.

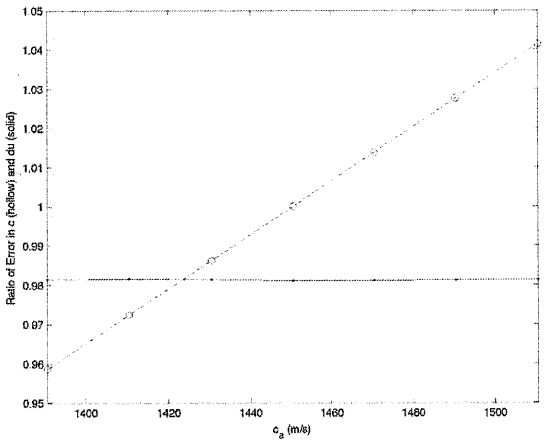

Figure 2: Ratio of along-track array element displacement to ideal displacement determined by the RPC method as a function of c_i (solid dots and line). ε is displayed for reference (circles, dashed line) to highlight the lack of response in RPC calculated displacement as a function of c_i.

2.3 Autofocus

The implemented autofocus algorithm operates by dividing the error-affected image into multiple strips varying in range. A two-dimensional modification to the classic mapdrift algorithm described in Carrera[5] was implemented to estimate the quadratic phase error. Wide-beam wide-band range-dependent quadratic phase error in the two-dimensional Fourier spectrum of each strip was modeled in polar coordinates as:

(9)

In Eq. (9) θ is the sonar look angle and k is radial wavenumber . Two windows are applied to the spectrum to gate around the drift squint angle $\pm\theta_s$. The windows are formed to place the centroids at k_{y_c}, = $k_0\cos(\theta_s)$, $k_{\pm x\_c} = \pm\, k_0\sin(\theta_s)$, and . To prevent biasing from uneven spectral distributions prewhitening can be applied:

, (10)

where S is the strip spectrum, is the whitened strip, and σ is a noise regulation parameter. For the present system this appears to work most effectively at Two-dimensional correlation with the intensity images formed by these sub-apertures is used to estimate an azimuthal translation (*i.e* "drift"). The drift value gives an estimate of the derivative of Q in the k_x direction at k_{y_c}, $k_{+/-x\_c}$. Expressing Q and its partial derivative with respect to k_x in Cartesian coordinates,

, (11)

. (12)

The second term is small relative to the first, and is neglected in the present case. At the strip having range r this derivative is known at (k_{y_c}, k_{x_c}) using the measured translation $P_x(r)$ pixels in the along-track direction:

, (13)

where k_{x_samp} is the azimuthal sample rate, typically 2π/du with du being the spacing of receiver phase centers. Eq. (13) can be substituted into (12) to solve for quadratic error $A(r)$ in terms of known values:

. (13)

A refocused image may be directly obtained by subtracting the estimated quadratic phase errors from the spectra of the strips and reverting to the spatial domain (this bypasses re-beamforming) however in the present case $A(r)$ is used to estimate an aperture synthesis parameter error. If the along-track spacing is accurately known then the dominant contribution to error can be attributed to error in propagation speed. For a strip at a given range $r_1 = t_1 c_i$ the new estimate can be obtained via solving for the value of c that makes the phase difference between the range and squint-range match the observed phase correction value. The squint-range phase difference at squint angle θ_s to a strip centered at t_1 is:

, (14)

where Q_{err} is the estimated error in radians at the centroid of the window and $\lambda = c_i/f_0$. Solving for c_{new} yields:

. (15).

Each range generates an independent estimate of c_{new} and using a quality estimate from the correlation coefficients found during drift estimation a weighted mean can be used to determine the sound speed.

2.4 Determination of c from autofocus results

The results presented in section 3 were achieved using the autofocus algorithm to determine c. An iterative process was required because some of the variables used to calculate the quadratic phase and updated value of c are themselves dependent on c (e.g. λ, θs, k0, k, r, etc). To test in-situ propagation speed estimation the value of c_i was blindly initialized at 1500 m/s. The RPC-based along track spacing error method described in section 2.1 was used to estimate a refined

sample spacing value, which was applied during beamforming. Following image formation and operating under the assumption that along-track spacing error has been made negligible the autofocus algorithm described in section 2.3 was applied to generate an update to the value of c. Sonar data was re-processed using the updated value of c, and following beamforming a further refinement was estimated using the autofocus algorithm. This process was repeated iteratively until the estimated sound speed correction converged to within 1 m/s. At this point the sonar-derived value for c was recorded (c_s). The process typically required 2 to 3 iterations.

3 EVALUATION OF ALGORITHM PERFORMANCE

A database of 26 samples of SAS data was compiled which contained data with system-recorded c values (otherwise referred to as assumed or c_a) ranging from 1450 – 1535 m/s. This data was selected to include a wide range of environmental conditions including temperature and salinity variations. The dataset also included shallow water areas where system motion and environmental conditions reduced RPC coherence, making RPC measurements challenging. The c_i value was initialized at 1500 m/s and c_s was determined for the database samples using the procedure described in section 2.4.

The results of the c_s value calculations are shown in Figure 3. The sonar measured values generally follow the system measured values, but the error is large. The mean ratio of sonar measured to system measured values is 1.001 indicating that the mean c_s value is within 0.1% of c_a, but the standard deviation of the ratio (0.008) indicates that the deviation of individual measurements are on the order of 1%. The difference between the two measurements ($c_a - c_s$) is small (2 m/s) with a standard deviation of 12 m/s.

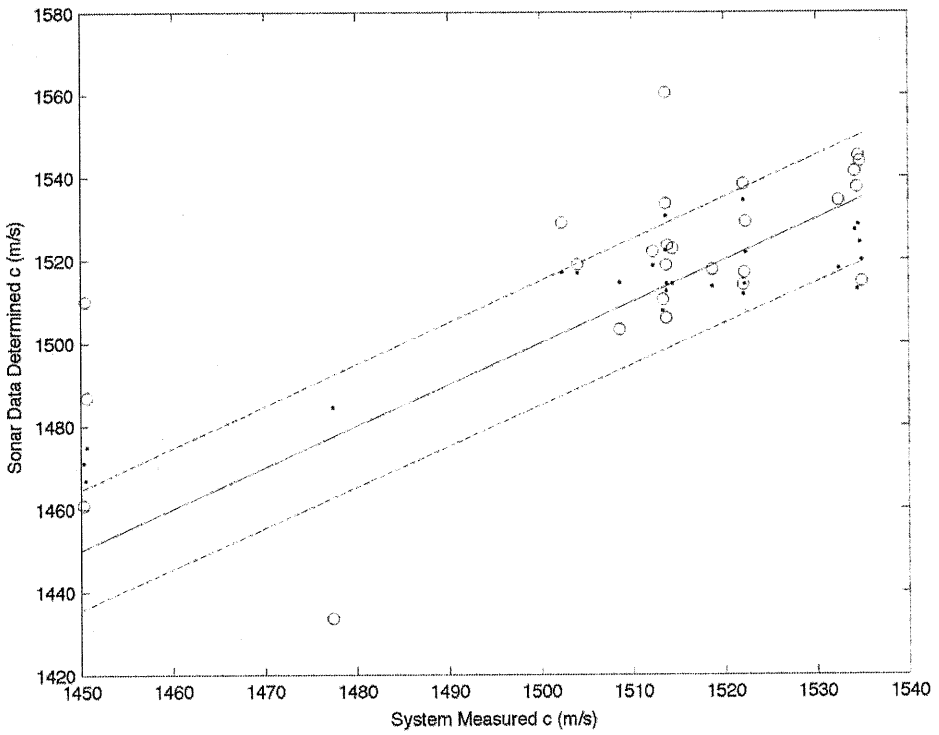

Figure 3: A comparison of system and sonar c measurements using the RPC along-track displacement measurement technique (solid) and using INS measurements for along-track displacement (hollow). The solid line represents a 1:1 relationship and the dashed lines indicate ±1% of the system measurement.

Figure 3 also shows the results from determination of c_s without using the RPC along-track technique. For this data, along-track motion compensation was provided from inertial navigation system (INS) measurements. These results indicate improved performance for RPC-based methods when comparing the two estimations of c_s. The INS-based measurements have significantly larger variance (mean ratio 1.005 ± 0.014).

While c_s values do contain error on the order of 1%, there were no discernable negative effects to image quality as indicated by visual inspection of the imagery even for cases where the initialization c_i value was in error by >100 m/s (Figure 4). This qualitative assertion is reinforced by review of estimates of the image resolution for imagery formed with the system measured and sonar measured c values. The ratio of the along-track resolution of the final imagery when using c_s to the final imagery when using c_a values is 1.00 ± 0.01, indicating that the resulting image resolution is with 1% within the range of c_i values tested (1400 m/s – 1600 m/s). It is important to point out here that imagery formed with c_a also had autofocus applied which corrected for linearly range variant quadratic phase error. Otherwise, the imagery formed with c_s would have had superior focus.

The consistency of c_s values was evaluated through the comparison of consecutive c measurements in a well-mixed environment. The selected data was collected in a shallow water open bay environment where c_a values were assumed to be stable due to turbulent mixing. Ten consecutive samples were evaluated for each of two adjacent transects. The transects consist of parallel paths ~40m apart with headings ~180° apart. The mean and standard deviation of c_a was 1522 ± 0.1 m/s indicating that the area is well mixed. The mean and standard deviation of c_s was 1535 ± 9 m/s. This is consistent with the previous result which showed ~1% standard deviation in c measurements, but the deviation from system measured c values is not zero mean. This may indicate that there is an additional factor contributing to the quadratic phase error (environmental or induced from errors in motion estimation), or may indicate that c_a includes a bias (i.e. the sensor used to determine c_a was not calibrated).

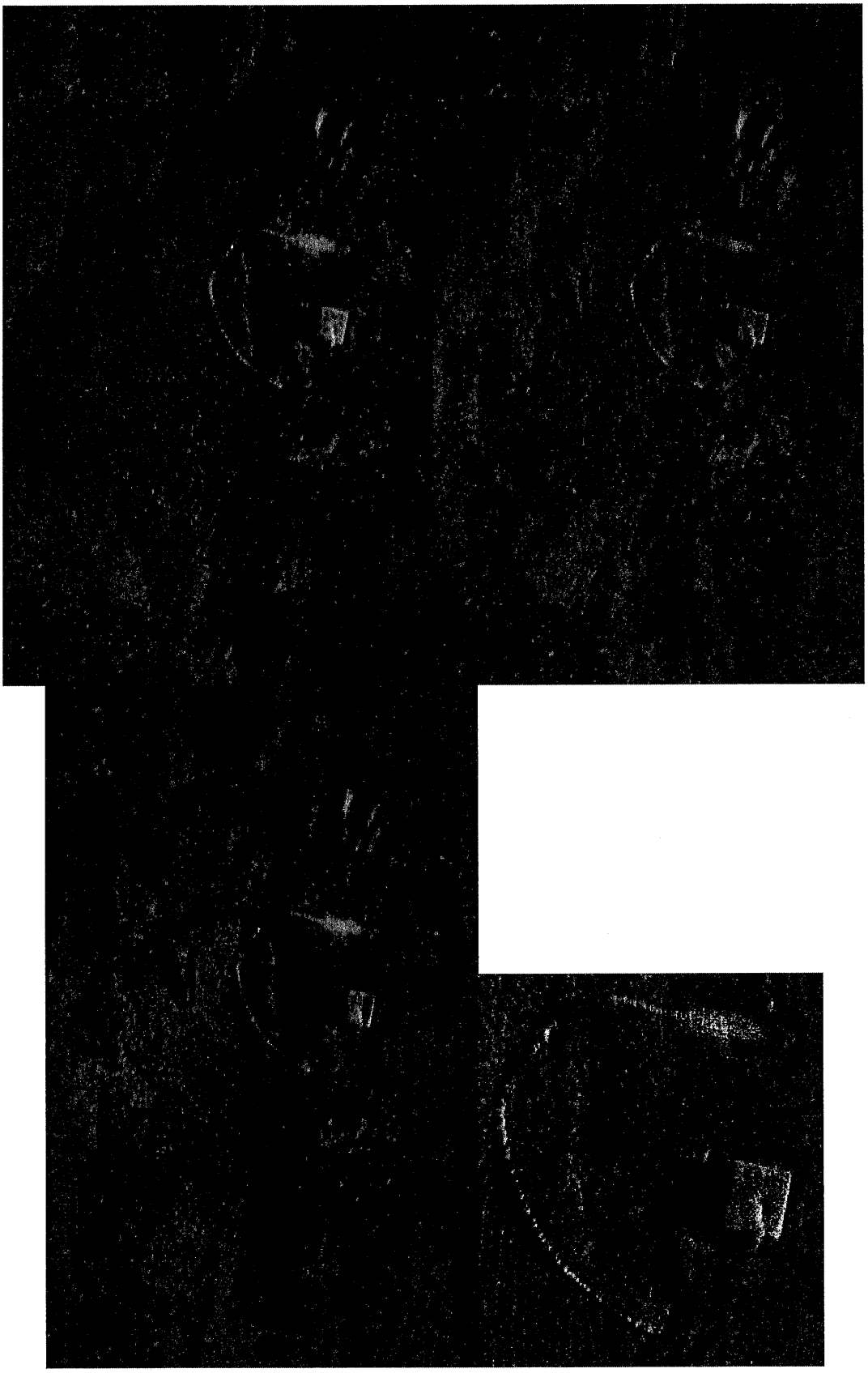

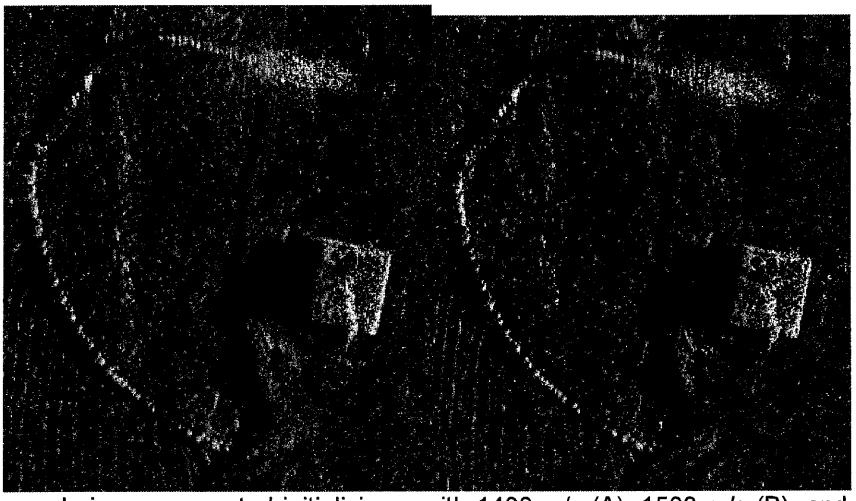

Figure 4: Example imagery created initializing c with 1400 m/s (A), 1500 m/s (B), and the system measured c value (C). An enlarged image including a concrete block and chain is included (lower row) for a closer inspection of focus.

4 CONCLUSIONS

SAS systems require accurate estimates of c in order to produce focused imagery. While most unmanned underwater vehicle systems provide onboard local estimates of c, systems operating at long ranges and in more complex environments require tools to determine or verify the *in situ* medium c value at ranges matching that of the system. In this paper, we describe a method to determine along-track position independent of c that can be used to improve sonar-based c measurements.

While the preliminary measurements described here contain significant error, it is clear that the precision of the measurement supports highly focused image formation. Further, it is important to point out that some of the c_a measurements that are assumed to be accurate for the purposes of this study may contain errors resulting from improper calibration and that the c_s values provide improved imagery focus. Additional testing is required where independent calibrated sensors are used during testing in order to collect data needed to definitively determine the efficacy of the method. If further analysis indicates that the technique provides estimates with large standard deviation but zero mean offset, larger samples can be utilized to minimize the sampling error and provide accurate results over a larger area.

Finally, the methods described here are not intended to provide the solution for long-range estimation of c, only to illustrate the potential use of SAS sensors to determine environmental parameters. Additional techniques should be developed that may provide measurements at increased spatial resolution, which could provide beneficial information for the acoustics community.

5 REFERENCES

1. D.A. Cook, "Synthetic Aperture Sonar Motion Estimation and Compensation", Thesis, Georgia Institute of Technology, May 2007.
2. S. Leier, J. Croen, A.M. Zoubir, U. Holscher, and I. Campbell, "The Influence of Sound Speed on Synthetic Aperture Sonar Imagery", Proceedings of the 1st International Conference and Exhibition on Underwater Acoustics, pp. 85–92, UAC, 2013.
3. A. Bellettini, and M.A. Pinto, "Theoretical Accuracy of Synthetic Aperture Sonar micronavigation Using a Displaced Phase-Center Antenna," IEEE Journal of Oceanic Engineering, vol.27 (4), 780-789, October 2002.

4 R.W. Sheriff, "Synthetic aperture beamforming with automatic phase compensation for high frequency sonars," in Proceedings of the 1992 Symposium on Autonomous Underwater Vehicle Technology, pp. 236–245, IEEE, 1992.

5. W.G. Carrara, R.S. Goodman, R.M. Majewski, "Spotlight Synthetic Aperture Radar: Signal Processing Algorithms." Artech House, 1995.